X-640-69-356
PREPRINT

NASA TM X-63670

STATIONARY WAVES PRODUCED BY THE EARTH'S BOW SHOCK

J. K. PEREZ
T. G. NORTHROP

AUGUST 1969

GSFC
GODDARD SPACE FLIGHT CENTER
GREENBELT, MARYLAND

STATIONARY WAVES PRODUCED BY THE EARTH'S BOW SHOCK

J. K. Perez

and

T. G. Northrop

Goddard Space Flight Center
Greenbelt, Maryland 20770

ABSTRACT

Stationary cyclotron waves attached to the bow shock are produced by the current in the shock. Waves upstream from the shock are circularly polarized electron waves, the polarization being in the sense of a right-hand screw when the interplanetary field is directed toward the shock, and left-hand when directed away. The downstream wave field has two components, one from the electron cyclotron branch and one from the ion cyclotron branch of the dispersion relation. The latter has a longer wavelength and a larger amplitude (by the ion/electron mass ratio) than the electron wave. It is elliptically polarized rather than circularly, and always in the opposite sense to the upstream electron wave. Therefore, the sense of polarization should be seen to reverse as the shock is traversed in either direction. When the ambient magnetic field is not perpendicular to the shock, there also exists a stationary electrostatic wave with its electric field normal to the shock. Both up-and downstream the ratio of the electrostatic wave to the magnetic wave amplitudes is of the order $u/c \tan \theta$, where θ is the angle between the normal to the shock and the magnetic field, and u is the plasma flow velocity.

I. Introduction

A thin current sheet was used in a previous paper [Tidman and Northrop, 1968] as a model for the bow shock and as a source of waves extending upstream and downstream from it. An example of these waves is reproduced in Fig. (1) from Heppner et al. [1966]. So long as the wavelengths are much larger than the thickness of the collisionless shock transition, it is unnecessary to examine the detailed mechanism of the shock that results in the sheet current. In Fig. (1) the bow shock is crossed at 2 min. 10 sec., where the amplitude and wavelength are seen to change suddenly.

Observed wavelengths [Fredricks, 1968] do not in fact always satisfy this condition, and work reported here must then be extended to be applicable. This present work makes predictions about the numerous shock crossings where the model does apply.

We use the same calculation method as in Tidman and Northrop [1968] but carry it further, in that we perform the integrations and obtain explicit expressions for the wave electric and magnetic fields. There only wavelengths were estimated and roughly compared to observations. We can now study the amplitude of these cyclotron waves, their ellipticity, if any, and the polarization sense for comparison with

observations. In addition we have considered a more general geometry than there by allowing the upstream and downstream flow vectors $\vec{u}_1$ and $\vec{u}_2$, and unperturbed magnetic fields $\vec{B}_1$ and $\vec{B}_2$ to be oblique to the shock. Thus the model applies everywhere in the ecliptic plane. Out the ecliptic plane is not covered because the flows and magnetic fields have been taken as coplanar with the normal to the shock. Extension to the most general case is not difficult, but we believe that the work reported carries this model as far as is reasonably worthwhile until comparison with experiment demonstrates its usefulness.

We consider only cases where the current $\vec{j}$ in the shock front is steady and normal to the ecliptic plane, as in Figure 2, where the x-axis is normal to the shock and the y-axis is normal to the ecliptic.

Tidman and Northrop [1968] gave consideration to the case where $\vec{j}$ is not steady, but we believe that extending the study to such cases with this model is again more appropriately postponed until comparison with observation indicates a need. Nevertheless, we give the formulation for non-steady currents.

In the frame of reference of the flowing plasma, the shock appears as a current sheet being moved in direction $-\vec{u}_{1,2}$ through the plasma. Because the magnetic field of the current $\vec{j}$ interacts with the plasma particles, the shock is an impediment to the plasma flow. Waves can be expected, just as in the case of a boat moving through the water. We can find expressions for the plasma waves by standard methods of analysis applied to the Vlasov-Maxwell system of equations, this being the valid set of equations for a collisionless plasma. This set is linearized about unperturbed values. For example $\vec{B}$ (upstream) = $\vec{B}_1 + \vec{B}_1^{(1)}$ where

$\vec{B}_1^{(1)}$ is the wave field. The wave amplitude is often observed to be comparable with $\vec{B}_1$, so that a linearized treatment may not always be quantitative. But the qualitative predictions we can make are likely to be correct.

We do the problem as an initial value problem in time, the sheet current being zero for $t < 0$. We also obtain the asymptotic form of the field as $t \to \infty$.

It is easiest to obtain the oblique flow case ($\Psi \neq 0$) from the normal flow ($\Psi = 0$) case via a Lorentz transformation to a frame sliding parallel to the shock. We therefore first obtain the wave fields in the shock rest frame for $\Psi_{1,2} = 0$, $\theta_{1,2} \neq 0$. It is easiest in turn to get these by first calculating the fields in the frame flowing with the plasma, where the plasma is at rest, and then making a Lorentz transformation to the shock rest frame. All of our results are presented in the shock frame, and are therefore time independent, the current having been assumed steady and the $t \to \infty$ limit used. A spacecraft moving through this stationary, nontime-dependent wave pattern will of course see time-dependent fields, as in Fig. (1).

II. Upstream fields for flow normal to shock and magnetic field oblique (ion mass taken as infinite)

This case is applicable to the subsolar point. By analysis similar to the Appendix of Tidman and Northrop [1968], we find the magnetic and electric fields in the shock frame to be:

$$\vec{B}_1^{(1)}(x,t) = -2i\sum_n e^{i\omega_n t}\int_{-\infty}^{\infty} dk_x e^{ik_x x}\left[\frac{(k_x - \frac{\omega_n u_1}{c^2})\,\hat{x}\times\vec{\vec{C}}\cdot\vec{j}_n}{\omega^2\,|\vec{\vec{K}}(\vec{k},\omega) - \frac{k^2c^2}{\omega^2}\vec{\vec{I}}_T|}\right]_{\substack{\omega = -\omega_n - k_x u_1 \\ k_y = k_z = 0}} \quad (1$$

$$\vec{E}_1^{(1)}(x,t) = 2i\sum_n e^{i\omega_n t}\int_{-\infty}^{\infty} dk_x e^{ik_x x}\left[\frac{(\omega_n\vec{\vec{I}} + k_x u_1 \hat{x}\hat{x})\cdot\vec{\vec{C}}\cdot\vec{j}_n}{\omega^2\,|\vec{\vec{K}}(\vec{k},\omega) - \frac{k^2c^2}{\omega^2}|}\right]_{\substack{\omega = -\omega_n - k_x u_1 \\ k_y = k_z = 0}} \quad (2$$

The sheet current has been taken as $\sum_{n=-\infty}^{\infty}\vec{j}_n e^{i\omega_n t}\delta(x)$ so as to permit arbitrary time dependence; $\vec{\vec{K}}(\vec{k},\omega)$ is the plasma dielectric tensor; $\vec{\vec{I}}_T$ is a unit dyadic perpendicular to $\vec{k}$; the vertical bars indicate the determinant; and $\vec{\vec{C}}$ is the transpose of the cofactor of the matrix $(\vec{\vec{K}} - \frac{k^2c^2}{\omega^2}\vec{\vec{I}}_T)$; $\hat{x}$ is a unit vector along the x-axis. The elements of $\vec{\vec{K}}$ are rather complicated, particularly when there is a magnetic field. $(\vec{\vec{K}} - \frac{k^2c^2}{\omega^2}\vec{\vec{I}}_T)$ is the same as $(-\frac{\vec{\vec{R}}}{\omega^2})$ in Montgomery and Tidman [1964, p. 139] and is also equal to the matrix given in Eq. (1-20) of Stix [1962, p. 11]. The ω, k_y, and k_z integrations have already been performed in inverting the transforms, leaving only the k_x integrations in (1) and (2). The $\vec{k}$ vector of the waves is normal to the shock. The plasma has been assumed stable, so that all zeroes of $\omega^2\,|\vec{\vec{K}} - \frac{k^2c^2}{\omega^2}\vec{\vec{I}}_T|$ are on or below the real axis in the ω plane. There will actually be damping due to finite

temperature in a stable plasma, so that at large times the damped solutions of $\omega^2 \left|\vec{\vec{K}} - \frac{k^2c^2}{\omega^2}\vec{\vec{I}}_T\right| = 0$ contribute nothing to the ω integration. We are assuming that the damping time of the least damped pole is much less than the smallest $1/\omega_n$, or in other words, that fluctuations in the sheet current occur in a time scale slow compared to the damping time. This assumption could need modification if high enough frequency fluctuations are present in the current sheet. The only pole that contributes to the ω integral at large times is an undamped one due to the plasma flow, it appears as a factor $(\omega + \omega_n + k_x u_1)$ in the denominator of the ω integrand.

To make this paper reasonably self-contained, we now reiterate a few salient points from Tidman and Northrop [1968]. The elements of $\vec{\vec{K}}$ for a cold plasma are algebraic and therefore $\omega^2 \left|\vec{\vec{K}}(\vec{k},\omega) - \frac{k^2c^2}{\omega^2}\vec{\vec{I}}_T\right|_{k_y=k_z=0}$ is of the form $f(k_x,\omega)\prod_{i=1}^{n}[\omega - \omega_i(k_x)]$, where $f(k_x, \omega)$ does not vanish for real k_x and ω. The $\omega_i(k_x)$'s are real. Fig. 3 is a sketch of $\omega_i(k_x)$. To simulate damping in this formally undamped plasma, $\omega_i(k_x)$ is replaced by $\omega_i(k_x) - i\epsilon$. The $i\epsilon$ is essential to determine which poles of the integrand in the k_x plane contribute to upstream and which to downstream waves. Poles of the k_x integrand are found by solving $-\omega_n - k_x u_1 - \omega_i(k_x) + i\epsilon = 0$. Solutions are $k_x = k_{ox} + \frac{i\epsilon}{u_1 + \frac{d\omega_i}{dk_{ox}}}$, where k_{ox} is a solution for $\epsilon = 0$.

The k_x integration for $x < 0$ - that is, for upstream waves, is performed by closing the contour at infinity in the lower half k_x plane, thus picking up contributions from any pole in the lower half plane. From Fig. 3, $d\omega_i/dk_{ox} < 0$; then because $u_1 + \frac{d\omega_i}{dk_{ox}}$ must be negative for a

solution k_{ox} to contribute to upstream waves, u_1 must be $< \left|\frac{d\omega_i}{dk_{ox}}\right|$ to get upstream waves. This makes sense physically: the group velocity (which is negative and therefore directed upstream) must be fast enough to beat the flow and allow energy to propagate upstream from the source. Similarly, the k_x integration contour for downstream waves closes in the upper half k_x plane and picks up contributions from k_{ox}'s for which $u_2 > \left|\frac{d\omega_i}{dk_{ox}}\right|$. The flow velocity downstream must be sufficiently large to sweep energy away from the shock in the downstream direction.

Considerable analysis is needed in connection with both the determinant and the $\vec{\vec{C}}$ in Eqn's (1) and (2). The elements of the determinant are given in (4) and (5) in a coordinate system with $\vec{B}$ along the z-axis, whereas in Fig. 2, $\vec{B}$ is oblique to the z-axis. Therefore a rotation of the matrix $(\vec{\vec{K}} - \frac{k^2c^2}{\omega^2}\vec{\vec{I}}_T)$ must be made. [See Appendix for details.] A second complication is that when $\vec{B}$ and $\vec{k}$ are oblique, longitudinal and transverse modes do not separate and factoring the determinant into the form $\prod_i [\omega-\omega_i(k_x)]$ requires the solution of an algebraic equation of high degree. Fortunately, if one expands in the ratio Ω_e/ω_e of gyro to plasma frequencies, this problem is eliminated. For the solar wind $\Omega_e/\omega_e \sim 10^{-3}$ upstream, and therefore the approximation should be excellent.

By use of Stix's [1962] equations (1-21) and (2-42) we have

$$\left|\vec{\vec{K}} - \frac{k^2c^2}{\omega^2}\vec{\vec{I}}_T\right| = A\left\{\frac{k^2c^2}{\omega^2} - 1 + \frac{2\left(1 - \frac{\omega_e^2}{\omega^2}\right)}{\frac{2\omega^2}{\omega_e^2}\left(1 - \frac{\omega_e^2}{\omega^2}\right) - \frac{\Omega_e^2}{\omega_e^2}\sin^2\theta + \frac{\Omega_e}{\omega_e}\left[\frac{\Omega_e^2}{\omega_e^2}\sin^4\theta + \frac{4\omega^2}{\omega_e^2}\left(1 - \frac{\omega_e^2}{\omega^2}\right)^2\cos^2\theta\right]^{\frac{1}{2}}}\right\}$$

$$\times\left\{\frac{k^2c^2}{\omega^2} - 1 + \frac{2\left(1 - \frac{\omega_e^2}{\omega^2}\right)}{\frac{2\omega^2}{\omega_e^2}\left(1 - \frac{\omega_e^2}{\omega^2}\right) - \frac{\Omega_e^2}{\omega_e^2}\sin^2\theta - \frac{\Omega_e}{\omega}\left[\frac{\Omega_e^2}{\omega_e^2}\sin^4\theta + \frac{4\omega^2}{\omega_e^2}\left(1 - \frac{\omega_e^2}{\omega^2}\right)^2\cos^2\theta\right]^{\frac{1}{2}}}\right\} \qquad (3)$$

where

$$A = \left(1 - \frac{\Omega_e^2}{\omega^2}\right)^{-1}\left(1 - \frac{\Omega_e^2}{\omega^2} - \frac{\omega_e^2}{\omega^2} + \frac{\omega_e^2\Omega_e^2}{\omega^4}\cos^2\theta\right); \qquad (4)$$

Ω_e is the electron gyro frequency and ω_e is the electron plasma frequency. In Eq.'s (3) and (4) the effect of ion motion on the waves has been neglected ($m_i = \infty$), because, as can be seen in Fig. 3, the upstream waves arise only from intersections with the electron branch when the flow velocity is greater than the Alfvén velocity. The finite ion mass does have a small effect on the electron branch, but this we ignore. When we consider downstream waves, the ion motion must be retained in order to obtain wavelengths longer than upstream, as in Fig. 2. From Fig. 3, $\omega_i(k_{ox}) \gtrsim \Omega_e$, so that $\frac{\omega_e^2}{\omega^2} \gtrsim \frac{\omega_e^2}{\Omega_e^2} \gg 1$. Thus in the approximation $\Omega_e^2/\omega_e^2 \ll 1$

$$A \simeq \left(\frac{\omega_e^2}{\Omega_e^2 - \omega^2}\right)\left(1 - \frac{\Omega_e^2}{\omega^2}\cos^2\theta\right) \qquad (5)$$

In the radicals in the curly-bracketed factors of Eq. (3), the first term $\frac{\Omega_e^2}{\omega_e^2}\sin^4\theta$ is dropped as small. This approximation is good so long as θ is not too close to $\Pi/2$, at which angle the second term is identically zero. However, for the solar wind "too close" is within about 10^{-5} radians of $\Pi/2$, so that the approximation is excellent in any practical case. To order

$\frac{\Omega_e}{\omega_e}$, Eq. (3) becomes

$$\left|\vec{\vec{K}} - \frac{k^2c^2}{\omega^2}\vec{\vec{I}}_T\right| \simeq \frac{\omega_e^2}{(\Omega_e^2-\omega^2)\omega^6}\left[k^2c^2(\omega-\Omega_e\cos\theta)+\omega\omega_e^2\right] \times \left[k^2c^2(\omega+\Omega_e\cos\theta)+\omega\omega_e^2\right], \qquad (6$$

where in addition 1 has been dropped compared to $\frac{k^2c^2}{\omega^2}$, which equals $\frac{c^2}{u_1^2}$.

For a steady sheet current, $\vec{j}_n = 0$ for $n \neq 0$, and $\omega_o = 0$, so that $\vec{j} = \vec{j}_o$ only. The quantity $\hat{x} \times \vec{\vec{C}} \cdot \vec{j}_o$ then appearing in the numerator of Eq. (1) is given in the Appendix. In the $\frac{\Omega_e}{\omega_e} \ll 1$ approximation it becomes (with $\vec{j}_o = \hat{y}\ j_y$)

$$\hat{x} \times \vec{\vec{C}} \cdot \vec{j}_o \cong \frac{\omega_e^2}{\omega^2}\left[\hat{z}\ \frac{k^2c^2(\omega^2-\Omega_e^2\cos^2\theta) + \omega_e^2\omega^2}{\omega^2(\omega^2 - \Omega_e^2)} + \hat{y}\ \frac{i\omega_e^2\Omega_e\cos\theta}{\omega(\omega^2 - \Omega_e^2)}\right] j_y \qquad (7$$

where again 1 has been dropped compared to k^2c^2/ω^2. Similarly in Eq. (2) (see Appendix)

$$k_x u_1 \hat{x}\hat{x} \cdot \vec{\vec{C}} \cdot \vec{j}_o = \hat{x}\ \frac{ik_x u_1 \omega_e^2 \Omega_e\ (\omega_e^2 + k^2c^2)\sin\theta}{\omega^3\ (\omega^2 - \Omega_e^2)}\ j_y \qquad (8$$

The zeros of the right hand side of (6) are needed, with ω set equal to $- k_x u_1 + i\varepsilon$, rather than the $- k_x u_1$ indicated in Equations (1) and (2),

for the following reason: $\left|\vec{\vec{K}} - \frac{k^2c^2}{\omega^2}\vec{\vec{I}}_T\right|$ is of the form $f(k_x,\omega)\prod_{i=1}^{n}[\omega-\omega_i(k_x)]$ where $\omega_i(k_x)$ must be replaced by $\omega_i(k_x) - i\varepsilon$ to include the damping and ω is to be replaced by $- k_x u_1$. Thus the damping can be equivalently introduced by writing ω as $- k_x u_1 + i\varepsilon$ and not modifying the $\omega_i(k_x)$. It is then unnecessary to write the determinant in explicitly factored form.

We therefore set $\omega = - k_x u_1 + i\varepsilon$ in (6) and solve for k_x. (The subscript x on k_x will be dropped from here on.) The first square bracket in Eq. (6) has zeros at k_1 and k_2, the second at k_3 and k_4, where

$$k_1 = - \frac{\Omega_e \cos\theta}{2u_1} + 1/2\left(\frac{\Omega_e^2\cos^2\theta}{u_1^2} - \frac{4\omega_e^2}{c^2}\right)^{1/2} \mp i\varepsilon$$

$$k_2 = - \frac{\Omega_e \cos\theta}{2u_1} - 1/2\left(\frac{\Omega_e^2\cos^2\theta}{u_1^2} - \frac{4\omega_e^2}{c^2}\right)^{1/2} \pm i\varepsilon \qquad (9)$$

$$k_3 = \frac{\Omega_e \cos\theta}{2u_1} + 1/2\left(\frac{\Omega_e^2\cos^2\theta}{u_1^2} - \frac{4\omega_e^2}{c^2}\right)^{1/2} \pm i\varepsilon$$

$$k_4 = \frac{\Omega_e \cos\theta}{2u_1} - 1/2\left(\frac{\Omega_e^2\cos^2\theta}{u_1^2} - \frac{4\omega_e^2}{c^2}\right)^{1/2} \mp i\varepsilon$$

The upper signs on the $i\varepsilon$ terms apply when $-\frac{\Pi}{2} < \theta < \frac{\Pi}{2}$, and the lower for $\frac{\Pi}{2} < \theta < \frac{3\Pi}{2}$. Very small regions around $\Pi/2$ and $3\Pi/2$ are excluded by our approximations, as stated previously. Some positive definite factors multiplying the $i\varepsilon$ terms have been omitted because they do not affect the overall sign of the term. We see that k_1 and k_4 give poles of the integrands in (1) and (2)

contributing to upstream waves, while k_2 and k_3 contribute to downstream (if u_1 is replaced by u_2) for $-\frac{\Pi}{2} < \theta < \frac{\Pi}{2}$. In other words, $u_1 + \frac{d\omega}{dk_o}$ is negative at k_1 and k_4.

The roots k_1 and k_2 merge and become complex when $\frac{\Omega_e^2 \cos^2\theta}{u_1^2} - \frac{4\omega_e^2}{c^2}$ goes negative. In Fig. 3 this happens when the line $\omega = -ku_1$ through the origin becomes tangent to the electron branch. This occurs if the solar wind velocity u_1 becomes too great, greater than about 700 km/sec for $\theta = 0$ (using the "standard" values for the solar wind given in the Appendix). It can also occur if the u_1 remains fixed and the angle θ between $\vec{B}_1$ and the shock normal increases beyond a critical value (about 55° by our standard values). Beyond the critical values the radical is imaginary and the waves are heavily damped, in just a few kilometers, in fact. Our standard upstream values make $\frac{2\Pi}{k_1} = \lambda_1 = 52$ km at $\theta = 0$.

It should be noted that in the $\Omega_e/\omega_e \ll 1$ expansion, the dispersion relation for the transverse waves (square brackets in (6)) for $\theta \neq 0$ are obtained from those for $\theta = 0$ by changing Ω_e to $\Omega_e \cos\theta$. One can imagine in Fig. 3, as θ is increased from zero, that the electron branch is reduced by $\cos\theta$, so that eventually it becomes tangent to $\omega = -ku_1$. (It is not, however, true that the elements of the matrix $\left(\overleftrightarrow{K} - \frac{k^2c^2}{\omega^2}\overleftrightarrow{I}_T\right)$ for $\theta \neq 0$ can be obtained from the $\theta = 0$ case by the same prescription.)

Both factors of A in (4) are independent of k and therefore represent non-dispersive waves, with zero group velocity, which cannot contribute to upstream waves.

We give no details of the k_x integrations, which are straightforward and require evaluation of residues at k_1 and k_4 for $-\frac{\Pi}{2} < \theta < \frac{\Pi}{2}$, and at k_2 and k_3 for $\frac{\Pi}{2} < \theta < \frac{3\Pi}{2}$. The explicit expressions (9) for k_1 and k_2 must be used after performing the integrations in order to show that the coefficients obtained for the $\hat{y}$ and $\hat{z}$ magnetic field components are in fact equal, although they appear quite different. Their equality establishes that the magnetic field is circularly polarized for all values of θ.

We find the following for the upstream fields:

For $-\frac{\Pi}{2} < \theta < \frac{\Pi}{2}$,

$$\vec{B}^{(1)}(x) = \frac{4\Pi u_1 \omega_e^2 j_y (\hat{y} \sin k_1 x + \hat{z} \cos k_1 x)}{(-k_1)c^2 (\Omega_e^2 c^2 \cos^2\theta - 4\omega_e^2 u_1^2)^{1/2}} \tag{10}$$

$$\vec{E}^{(1)}(x) = \frac{4\Pi u_1^2 (\omega_e^2 + k_1^2 c^2) j_y \tan\theta \, \hat{x} \sin k_1 x}{k_1 c^3 (\Omega_e^2 c^2 \cos^2\theta - 4\omega_e^2 u_1^2)^{1/2}} \tag{11}$$

and for $\frac{\Pi}{2} < \theta < \frac{3\Pi}{2}$,

$$\vec{B}^{(1)}(x) = \frac{4\Pi u_1 \omega_e^2 j_y (\hat{y} \sin k_2 x + \hat{z} \cos k_2 x)}{k_2 c^2 (\Omega_e^2 c^2 \cos^2\theta - 4\omega_e^2 u_1^2)^{1/2}} \tag{12}$$

$$\vec{E}^{(1)}(x) = \frac{4\Pi u_1^2 (\omega_e^2 + k_2^2 c^2) j_y \tan\theta \, \hat{x} \sin k_2 x}{(-k_2)c^3 (\Omega_e^2 c^2 \cos^2\theta - 4\omega_e^2 u_1^2)^{1/2}} \tag{13}$$

Eq. (9) gives k_1 and k_2. The ic can now be omitted.

Several important conclusions are to be drawn from these expressions:

1. An electrostatic field is present when the magnetic field is oblique to the shock normal ($\theta \neq 0$). The ratio of the electric to the magnetic field amplitude is $u_1(\omega_e^2 + k_1^2c^2) \tan\theta/\omega_e^2 c$. Because k_1^2 increases with θ, the maximum value of the ratio occurs at the maximum θ ---i.e., θ_c. Our standard values make this maximum ratio about $3\ u_1/c$. Thus the ratio will always be $\lesssim 3u_1/c$ upstream.
2. The magnetic field is circularly polarized in a right-hand screw sense about the component of unperturbed field normal to the shock, when that component is directed towards the shock. It is left-hand polarized when the field is directed generally away from the shock. The $\vec{B}^{(1)}$ is illustrated in Fig. 4 for both cases.
3. Reversing the unperturbed magnetic field (i.e. changing θ to $\Pi + \theta$) reverses the sense of the polarization, as just stated, but the amplitude remains unchanged.
4. The fields become infinite at either the critical angle or critical flow velocity - that is, when $(\Omega_e^2c^2 \cos^2\theta - 4\omega_e^2u_1^2) = 0$. The physical interpretation is that at the critical condition the group velocity equals the flow velocity so that wave energy radiated by the bow shock cannot move away from it and therefore builds up in amplitude. Of course, the result is not to be taken too seriously, because linearization will become invalid. However, one might expect to see larger fields when conditions are near critical.

III. Upstream fields for flow and magnetic field both oblique (ion mass taken infinite)

At a point in the ecliptic plane not at the subsolar point, the plasma flow and magnetic field are both oblique to the shock, as in Fig. 2. If there is a current sheet only in the shock frame, there will in general be both a current sheet and a charge sheet seen in other frames, in particular in the frame in which the plasma is at rest. This charge is of order u_1/c and is obtained from the charge-current four vector [Jackson, 1962, p. 378]. The entire problem could be redone, including now the test charge sheet, which one expects will excite electrostatic waves. Fortunately, the order u_1/c charge eventually has only an order u_1^2/c^2 effect on the fields. Because we are not working to this order, the charge can be ignored. Moreover, for the case we consider, where $\vec{j}$ is normal to the ecliptic and therefore perpendicular to $\vec{u}_1$, there is no charge to order u_1/c even.

The easiest way to obtain the fields for the oblique flow case is to make a Lorentz transformation in the ecliptic plane in a direction parallel to the shock plane; the oblique flow then becomes a normal flow, for which we already have the fields. Because there is no charge in the shock frame, the current in any other frame is the same through order u_1/c, so that j_y can be taken as unchanged when making the Lorentz transformation. The situation in the two frames of reference is as in Fig. 5, where the plane of the page is the ecliptic plane. The magnitude and angle of the magnetic field to the normal have been indicated by the primes as being different in the two frames. There are unperturbed electric fields in Figs. 2 and 5 normal to the ecliptic that

permit the plasma to flow at an angle to the magnetic field. When there is an electric field in one frame, the magnetic field in another frame differs in order u_1/c from that in the original frame [Jackson, 1962, p. 380]. However, the electric field $\vec{E}_1$ in the shock frame is $(u_1/c)\, B_1 \sin(\theta_1 - \Psi_1)$ into the page. Because it is already of order u_1/c, its effect on $\vec{B}_1$ is of order u_1^2/c^2 and negligible. So $\theta_1' = \theta_1$ and $\vec{B}_1' = \vec{B}_1$. (The electric field $E_1' = (u_1/c)B_1 \sin\theta \cos\beta$. We will not need to use it, however.)

Equations (10)-(13) give us the fields in the normal flow frame of Fig. 5, provided we replace u_1 in those equations by the applicable normal flow velocity here - namely, $u_1 \cos\Psi_1$. We then make a Lorentz transformation to a frame moving at $u_1 \sin\Psi_1$ in the negative z direction, as shown, and the resulting fields are those seen from the shock frame of Fig. 5. The transformation is straightforward, the vector form given for example in Jackson [1962, p. 380] being easy to use. The relations between the wave fields in the two frames of Fig. 5 are found to be:

$$\vec{E}^{(1)} = \hat{x}\left[E_x^{(1)'} + \frac{u_1 \sin\Psi_1}{c}\, B_y^{(1)'}\right] \tag{14}$$

$$\vec{B}^{(1)} = \vec{B}^{(1)'} + \hat{y}\,\frac{u_1 \sin\Psi_1}{c}\, E_x^{(1)'} \tag{15}$$

where the prime means in the normal flow frame and the subscript specifies the component. From equations (10) and (11) (for $-\Pi/2 < \theta < \Pi/2$)

$$\vec{E}^{(1)'} = \hat{x}\,\frac{4\Pi j_y u_1^2 \cos^2\Psi_1(\omega_e^2 + k_1^2c^2)\tan\theta_1 \sin k_1x}{k_1c^3\,(\Omega_e^2c^2\cos^2\theta_1 - 4\omega_e^2u_1^2\cos^2\Psi_1)^{1/2}} \tag{16}$$

$$\vec{B}^{(1)'} = \frac{4\Pi j_y u_1 \cos\Psi_1\omega_e^2(\hat{y}\sin k_1x + \hat{z}\cos k_1x)}{(-k_1)c^2(\Omega_e^2c^2\cos^2\theta_1 - 4\omega_e^2u_1^2\cos^2\Psi_1)^{1/2}} \tag{17}$$

and similarly from (12) and (13) for $\Pi/2 < \theta < 3\Pi/2$. Note that $\vec{E}^{(1)'}$ is of order u_1/c smaller than $\vec{B}^{(1)'}$, so that the second term on the right hand side of (15) may be dropped and $\vec{B}^{(1)} = \vec{B}^{(1)'}$. The wave fields for the oblique flow case are then:

For $-\Pi/2 < \theta < \Pi/2$

$$\vec{B}^{(1)} = \frac{4\Pi j_y u_1 \cos\Psi_1\omega_e^2(\hat{y}\sin k_1x + \hat{z}\cos k_1x)}{(-k_1)c^2(\Omega_e^2c^2\cos^2\theta_1 - 4\omega_e^2u_1^2\cos^2\Psi_1)^{1/2}} \tag{18}$$

$$\vec{E}^{(1)} = \frac{4\Pi j_y u_1^2 \cos\Psi_1\left[\omega_e^2\sin(\theta_1-\Psi_1) + k_1^2c^2\cos\Psi_1\sin\theta_1\right]\hat{x}\sin k_1x}{k_1\,c^3\cos\theta_1\,(\Omega_e^2c^2\cos^2\theta_1 - 4\omega_e^2u_1^2\cos^2\Psi_1)^{1/2}} \tag{19}$$

and for $\Pi/2 < \theta < 3\Pi/2$

$$\vec{B}^{(1)} = \frac{4\Pi\, j_y\, u_1 \cos\Psi_1\,\omega_e^2(\hat{y}\sin k_2x + \hat{z}\cos k_2x)}{k_2c^2\,(\Omega_e^2c^2\cos^2\theta_1 - 4\omega_e^2\,u_1^2\cos^2\Psi_1)^{1/2}} \tag{20}$$

$$\vec{E}^{(1)} = \frac{4\Pi j_y u_1^2 \cos \Psi_1 \left[\omega_e^2 \sin(\theta_1 - \Psi_1) + k_2^2 c^2 \cos \Psi_1 \sin \theta_1\right] \hat{x} \sin k_2 x}{(-k_2) c^3 \cos \theta_1 \left(\Omega_e^2 c^2 \cos^2 \theta_1 - 4\omega_e^2 u_1^2 \cos^2 \Psi_1\right)^{1/2}} \qquad (21)$$

where $k_{1,2} = -\frac{\Omega_e \cos \theta_1}{2u_1 \cos \Psi_1} \pm 1/2 \left(\frac{\Omega_e^2 \cos^2 \theta_1}{u_1^2 \cos^2 \Psi_1} - \frac{4\omega_e^2}{c^2}\right)^{1/2}$, the upper sign giving k_1 and the lower k_2.

The magnetic fields (18) and (20) for oblique flow can be obtained from the normal flow case (10) and (12) by changing u_1 to $u_1 \cos \Psi$. There is no corresponding simple prescription for the electric fields. The polarization of the wave remains circular with oblique flow. Indeed if $\Psi_1 = \theta_1$ or $\Pi + \theta_1$, so that the flow and unperturbed field vectors are parallel or antiparallel, the magnetic wave fields are independent of Ψ and θ; for if $\cos \Psi_1 = \cos \theta_1$, (18) becomes independent of the angles, as does k_1. Similarly for (20) if $\cos \Psi_1 = - \cos \theta_1$.

The critical condition for oblique flow is reached when the radical in the denominators vanishes. As one moves along the bow shock from the subsolar point towards the dawn or dusk meridian, the angle between the solar wind and the magnetic field remains fixed (at about 45°) while their angles to the normal changes. For the standard solar wind parameters, we find that there should be upstream waves from the subsolar point to the dawn meridian, but only for about 10° away from the subsolar point towards the dusk meridian. The magnetic field is not steady at 45° to the solar wind, but fluctuates in magnitude and direction. Therefore the 10° limit is not to be regarded too rigorously - only the qualitative prediction that upstream stationary waves should be less frequently observed on the dusk side.

IV. Downstream fields for flow normal to shock and magnetic field oblique

The downstream case is more difficult than the upstream to treat realistically because the plasma is no longer cold. The kinetic energy of flow has been converted to thermal energy by the shock. The conservation of mass, momentum, and energy equations relate the downstream conditions to the upstream. Nevertheless we can analyse the downstream waves independently of the upstream (realizing that the downstream unperturbed quantities are related to those upstream) by taking the downstream conditions as given. We also use the cold plasma dispersion dielectric tensor downstream with the belief that the principal qualitative result is valid. A warm plasma approximation could of course be used, but this again we believe ought to wait until need for more refined theory should become apparent from experimental observations.

In Fig. 3, the electron and ion branches are tangent at the origin when $\theta = 0$, their common slope being the Alfvén velocity. In the infinite ion mass approximation of Sections II and III, the Alfvén velocity is zero, so that the ion branch disappears into the horizontal axis, and the slope of the electron branch becomes zero at the origin. The downstream intersection with the electron branch will clearly give a shorter wavelength than the upstream, because $|k_2| > |k_1|$. This is at variance with Fig. 1. Indeed for our standard downstream conditions, the downstream wavelength would be 0.3 km, while the upstream wavelength is 52 km. The downstream electron wave is (for $-\frac{\Pi}{2} < \theta < \frac{\Pi}{2}$ and ion mass = ∞).

$$\vec{B}_2(1) = \frac{4\Pi j_y u_2 \omega_e^2 (\hat{y} \sin k_2 x + \hat{z} \cos k_2 x)}{(- k_2) c^2 (\Omega_e^2 c^2 \cos^2\theta_2 - 4\omega_e^2 u_2^2)^{1/2}} \qquad (22)$$

where k_2 is as in (9), but with downstream parameters, such as the downstream plasma frequency, etc. This downstream wave may be present, but clearly is not being seen in magnetometer records such as Fig. 1. The only way to get a longer wavelength downstream is from the ion branch. In order for the line $\omega = - ku_2$ to intersect the ion branch, u_2 must be less than the downstream Alfvén velocity (when $\theta_2 = 0$), or as we will see, u_2 must be $< v_A|\cos\theta|$ in general, where $v_A = \Omega_i c/\omega_i$.

Expressions (1) and (2) remain valid for downstream fields, if downstream quantities are used. We again find that approximating the elements of the matrix $(\vec{\vec{K}} - \frac{k^2c^2}{\omega^2} \vec{\vec{I}}_T)$ is essential to make the algebra tractable. We take the limit $m_e \to 0$. This limit does not eliminate the electrons from the picture; they still carry current. What it does is move the horizontal asymptote of the electron branch at Ω_e to infinity in Fig. 3, so that the line $\omega = - ku_2$ would never intersect the electron branch.

The oblique $\vec{B}_2$ necessitates rotation of the matrix again, just as in Section II, in order to evaluate the numerator of (1). We make the approximations that Ω_e/ω_e and Ω_i/ω_i are small, being about 10^{-2} and 10^{-3} respectively downstream. The determinant $|\vec{\vec{K}} - \frac{k^2c^2}{\omega^2} \vec{\vec{I}}_T|$ becomes

$$\left|\vec{\vec{K}} - \frac{k^2c^2}{\omega^2}\vec{\vec{I}}_T\right| = -\frac{\omega_e^2}{\omega^6(\omega^2-\Omega_i^2)}\left[k^4c^4(\omega^2-\Omega_i^2)\cos^2\theta_2+k^2c^2\omega^2\omega_i^2(1+\cos^2\theta_2)-\frac{\omega^4\omega_i^4}{\Omega_i^2}\right] \quad (23)$$

If we set (23) equal to zero, with $\omega = -ku_2 + i\varepsilon$, we find $k = k_o + i\varepsilon k_\varepsilon$ where

$$k_o^2 = \frac{\Omega_i^2}{u_2^2} + \frac{\omega_i^2 u_2^2}{\Omega_i^2 c^4 \cos^2\theta_2} - \frac{\omega_i^2(1+\cos^2\theta_2)}{c^2\cos^2\theta_2} \quad (24)$$

$$k_\varepsilon = \frac{c^4\Omega_i^4\cos^2\theta_2 - \omega_i^4 u_2^4}{u_2^3\Omega_i^2 c^4 k_o^2\cos^2\theta_2}$$

k_ε is always > 0 when $\cos^2\theta_2$ is such that $k_o^2 > 0$; $k_o^2 > 0$ when $u_2^2 < v_A^2\cos^2\theta_2$. This means that k_o always gives a downstream wave. The square bracket in (23) gives the ion and electron branches in the present approximations (See Fig. 6). When $\theta_2 \neq 0$, the ion and electron branches are no longer tangent.

Evaluation of the integral is again straightforward, there being two poles, at k_o and $-k_o$. The downstream wave from the ion branch is

$$\vec{B}^{(1)}(x) = \frac{-4\Pi\,\omega_i^2\,j_y}{k_o^2 c^3\,\omega_e^2\cos^2\theta_2}\Big\{\Big[\omega_e^2\,(2+\cos^2\theta_2-\frac{u_2^2}{v_A^2}) + \omega_i^2\,(\frac{v_A^2}{u_2^2}\sin^2\theta_2-\tan^2\theta_2)(1-\frac{u_2^2}{v_A^2})\Big]\,\hat{z}\cos k_o x + \hat{y}\,\frac{k_o u_2\cos\theta_2(\omega_e^2+2k_o^2c^2\sin^2\theta_2)}{\Omega_i}\sin k_o x\Big\} \qquad (25)$$

Eq. (25) is valid for all θ_2. The coefficient of cos $k_o x$ can be shown to be positive for all θ_2 such that $\cos^2\theta_2 > u_2^2/v^2_A$ that is, whenever there is downstream wave. The polarization about the x-axis is that of a left-hand screw when $-\Pi/2 < \theta < \Pi/2$ and right-hand otherwise. Therefore the rule of thumb for both upstream and downstream waves is: when the magnetic field is pointed generally away from the shock, the polarization is left hand about the x-axis, and when toward the shock, the polarization is right hand. Because the normal component of $\vec{B}$ is conserved across the shock, the upstream and downstream waves should always be oppositely polarized.

The wave in (25) is elliptically polarized. For $\theta_2 = 0$, the ratio of the $\hat{z}$ component to the $\hat{y}$ component is $(3 - u_2^2/v^2_A)/(1 - u_2^2/v^2_A)$. The polarization is thus very large for u_2 close to v_A, and very sensitive to u_2/v_A. The downstream waves thus should show rather large ellipticity.

There is an electrostatic downstream field when $\theta_2 \neq 0$, given by

$$\vec{E}^{(1)} = \frac{4\Pi\,j_y\,u_2^2\sin\theta_2\,(\omega_e^2+k_o^2c^2)\,\hat{x}\sin k_o x}{k_o\Omega_e\,c^4\cos^2\theta_2} \qquad (26)$$

The ratio of this electric field amplitude to the $\hat{y}$ component (which is the smaller component) of the magnetic field is of the order $\frac{u_2 \tan \theta_2}{c}$.

Finally, the relative amplitude of the downstream electron wave (22) to the downstream ion wave can be compared. The electron wave is about Ω_i/Ω_e smaller than $B_z^{(1)}$ in (25).

Appendix I - Evaluation of $\vec{\vec{C}}$

The elements of the tensor $(\vec{\vec{K}} - \frac{k^2c^2}{\omega^2}\vec{\vec{I}}_T)$ are given in Montgomery and Tidman [1964] in a coordinate system with the magnetic field along the z-axis. We have the field at an angle $(\Pi/2 - \theta)$ to the z-axis. Our tensor $\vec{\vec{C}}$ is related to the transposed cofactor of Montgomery and Tidman's tensor, by $C_{ij} = a_{mi}\, a_{nj}\, M_{ij}$, where M_{ij} is Montgomery and Tidman's transposed cofactor; a is the rotation matrix about the y-axis:

$$a = \begin{pmatrix} \sin\theta & 0 & \cos\theta \\ 0 & 1 & 0 \\ -\cos\theta & 0 & \sin\theta \end{pmatrix}$$

The numerators of the integrands in (1) and (2) are easily shown to be:

$$\hat{x} \times \vec{\vec{C}} \cdot \vec{j}_n = \hat{z}\,(j_{ny}\, C_{yy} + j_{nz}\, C_{yz}) - \hat{y}\,(j_{ny}\, C_{zy} + j_{nz}\, C_{zz})$$

$$(\omega_n \vec{\vec{I}} + k_x u_1\, \hat{x}\,\hat{x}) \cdot \vec{\vec{C}} \cdot \vec{j}_n = \hat{x}\,(\omega_n + k_x u_1)(j_{ny}\, C_{xy} + j_{nz}\, C_{xz})$$

$$\hat{y}\,\omega_n\,(C_{yy}\, j_{ny} + C_{yz}\, j_{nz})$$

$$+ \hat{z}\,\omega_n\,(C_{zy}\, j_{ny} + C_{zz}\, j_{nz})$$

Because we take $\omega_n = 0$, and because we consider only the case of sheet currents normal to the ecliptic, j_{nz} all vanish and

$$\hat{x} \times \overleftrightarrow{C} \cdot j_o = j_y \, (\hat{z} \, C_{yy} - \hat{y} \, C_{zy})$$

$$k_x u_1 \hat{x}\hat{x} \cdot \overleftrightarrow{C} \cdot \vec{j}_o = j_y \, k_x u_1 \, \hat{x} \, C_{xy}$$

Therefore only the three elements of C_{xy}, C_{yy}, and C_{zy} are needed. We find them to be

$$C_{xy} = M_{xy} \sin\theta + M_{zy} \cos\theta$$

$$C_{yy} = M_{yy}$$

$$C_{zy} = - M_{xy} \cos\theta + M_{zy} \sin\theta.$$

Thus in turn we need only M_{xy}, M_{yy}, and M_{zy}, which are easily obtained by taking the cofactor transposed of $- \overleftrightarrow{R}/\omega^2$ in Montgomery and Tidman. We find

$$M_{xy} = \frac{-i\omega_e^2 \, \Omega_e}{\omega(\omega^2 - \Omega_e^2)} \quad \left(1 - \frac{\omega_e^2}{\omega^2} - \frac{k^2c^2}{\omega^2} \sin^2\theta\right)$$

$$M_{yy} = \left(1 - \frac{\omega_e^2}{\omega^2}\right)\left(1 - \frac{k^2c^2}{\omega^2} - \frac{\omega_e^2}{\omega^2 - \Omega_e^2}\right) + \frac{k^2c^2}{\omega^2} \, \frac{\omega_e^2 \, \Omega_e^2}{\omega^2(\omega^2 - \Omega_e^2)} \sin^2\theta$$

$$M_{zy} = \frac{i \, \omega_e^2 \, \Omega_e}{\omega(\omega^2 - \Omega_e^2)} \, \frac{k^2c^2}{\omega^2} \cos\theta \sin\theta$$

and finally

$$\hat{x} \times \overleftrightarrow{C} \cdot \vec{j}_o = \left(1 - \frac{\omega_e^2}{\omega^2}\right) \left\{ \hat{z} \left[\left(1 - \frac{k^2c^2}{\omega^2} - \frac{\omega_e^2}{\omega^2 - \Omega_e^2}\right) + \frac{k^2c^2}{\omega^2} \frac{\omega_e^2 \Omega_e^2 \sin^2\theta}{\omega^2(\omega^2 - \Omega_e^2)(1 - \omega_e^2/\omega^2)} \right] \right.$$

$$\left. - \hat{y} \frac{i \omega_e^2 \Omega_e \cos\theta}{\omega(\omega^2 - \Omega_e^2)} \right\} j_y$$

$$k_x u_1 \hat{x} \hat{x} \cdot \overleftrightarrow{C} \cdot \vec{j}_o = - \hat{x} \frac{i k_x u_1 \omega_e^2 \Omega_e \sin\theta \left(1 - \frac{\omega_e^2}{\omega^2} - \frac{k^2c^2}{\omega^2}\right)}{\omega(\omega^2 - \Omega_e^2)}$$

Appendix II - Standard Values

Upstream		Downstream	
$\lvert\vec{B}_1\rvert$	$= 3 \times 10^{-5}$ gauss	$\lvert\vec{B}_2\rvert$	$= 12 \times 10^{-5}$ gauss
n_1	$= 4\ cm^{-3}$	n_2	$= 9\ cm^{-3}$
u_1	= 400 km/sec	u_2	= 100 km/sec
ω_e	$= 1.1 \times 10^{5}\ sec^{-1}$	ω_e	$= 1.7 \times 10^{5}\ sec^{-1}$
ω_i	$= 2.6 \times 10^{3}\ sec^{-1}$	ω_i	$= 3.9 \times 10^{3}\ sec^{-1}$
Ω_e	$= 5.3 \times 10^{2}\ sec^{-1}$	Ω_e	$= 2.1 \times 10^{3}\ sec^{-1}$
Ω_i	$= 2.9 \times 10^{-1}\ sec^{-1}$	Ω_i	$= 1.1\ sec^{-1}$
v_A	= 33 km/sec	v_A	= 88 km/sec

REFERENCES

Tidman, D. A., and T. G. Northrop, Emission of plasma waves by the earth's bow shock, J. Geophys. Res., 73, 1543, 1968.

Heppner, J. P., M. Sugiura, T. L. Skillman, B. G. Ledley and M. Campbell, OGO-A magnetic field observations, J. Geophys. Res., 71, 1481, 1966.

Montgomery, D. C., and D. A. Tidman, Plasma Kinetic Theory, McGraw-Hill, New York, 1964.

Stix, T. H., The Theory of Plasma Waves, McGraw-Hill, New York, 1962.

Jackson, J. D., Classical Electrodynamics, John Wiley & Sons, New York, 1962.

Fredricks, R. W., and P. J. Coleman, Jr., Observations of the microstructure of the earth's bow shock, to be published in the Proceedings of the International Conference on Plasma Instabilities in Astrophysics, 1968.

Figure Captions

Figure 1 The bow shock with coherent waves of frequencies near 1 cps, observed on November 25, 1964. Scales both uncorrected (the farthest left) and corrected for the spacecraft field are given. The 12-second periodicity is the satellite spin.

Figure 2 Geometry of the problem

Figure 3 Dispersion diagram (schematic) for $\vec{k}$ parallel to $\vec{B}$

Figure 4 Polarization of the upstream wave

Figure 5 Frames of reference for the oblique flow case

Figure 6 Downstream dispersion diagram (schematic) in the approximation where $m_e \to 0$

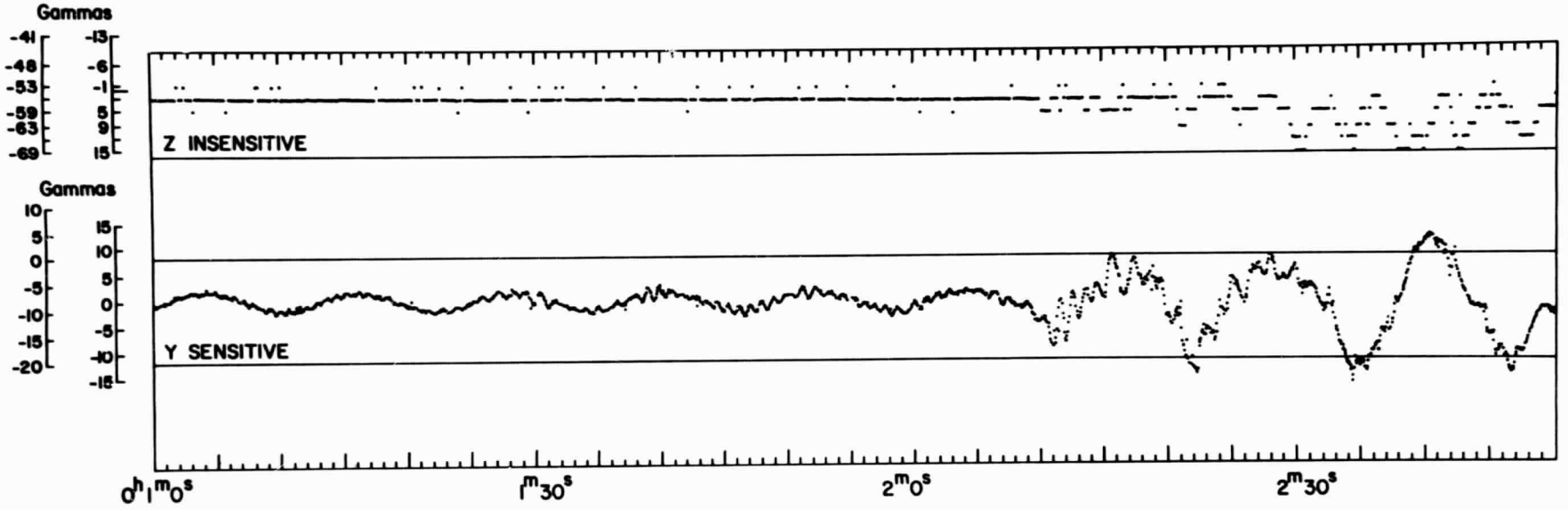
Gammas
-41
-48
-53
-59
-63
-69
-13
-6
-1
5
9
15
Z INSENSITIVE
Gammas
10
5
0
-5
-10
-15
-20
15
10
5
0
-5
-10
-15
Y SENSITIVE
0h1m0s
1m30s
2m0s
2m30s

FIGURE 1

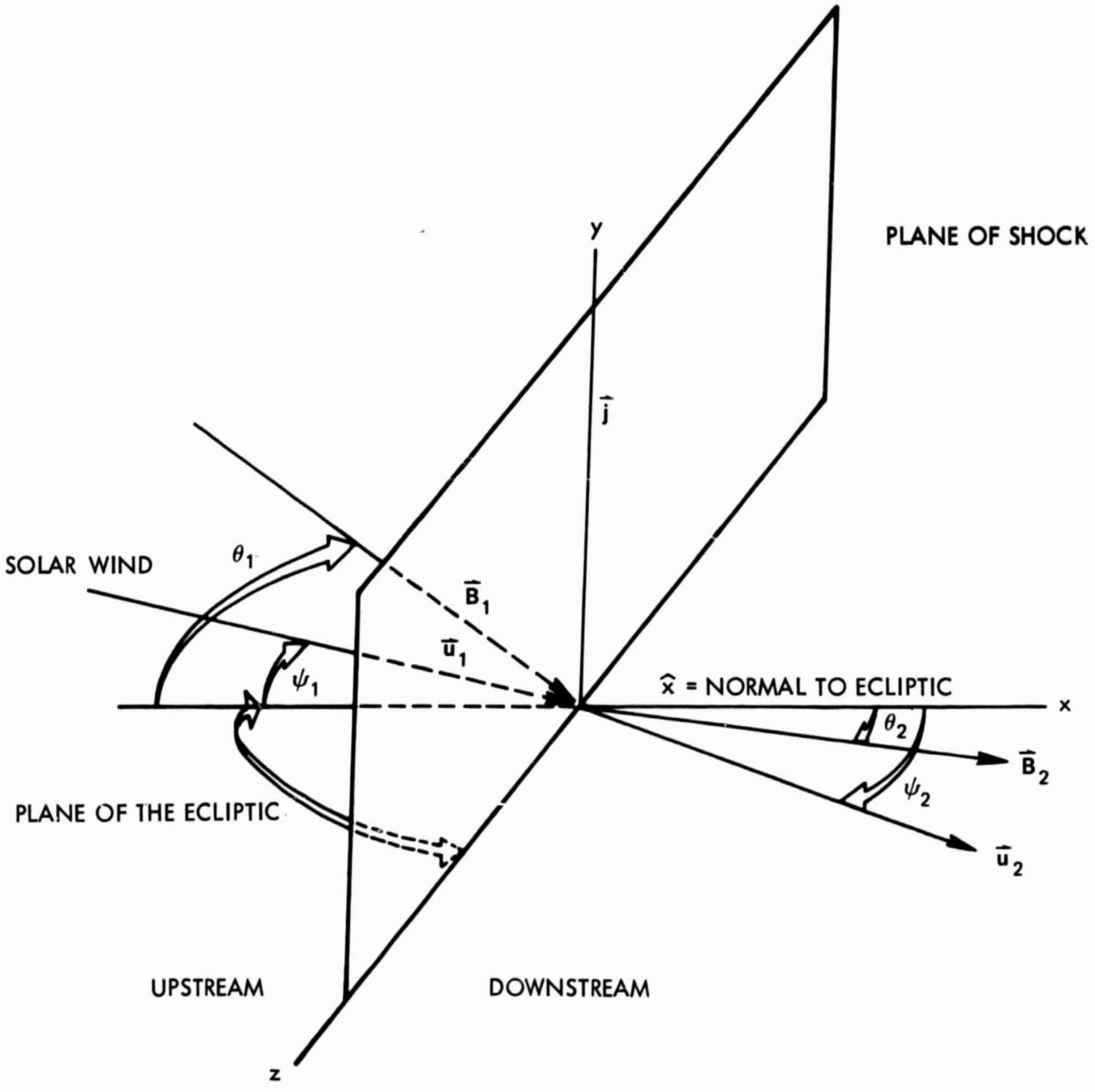
PLANE OF SHOCK
y
$\hat{j}$
SOLAR WIND
θ_1
$\hat{B}_1$
$\hat{u}_1$
ψ_1
$\hat{x}$ = NORMAL TO ECLIPTIC
x
θ_2
$\hat{B}_2$
ψ_2
$\hat{u}_2$
PLANE OF THE ECLIPTIC
UPSTREAM
DOWNSTREAM
z

FIG. 2

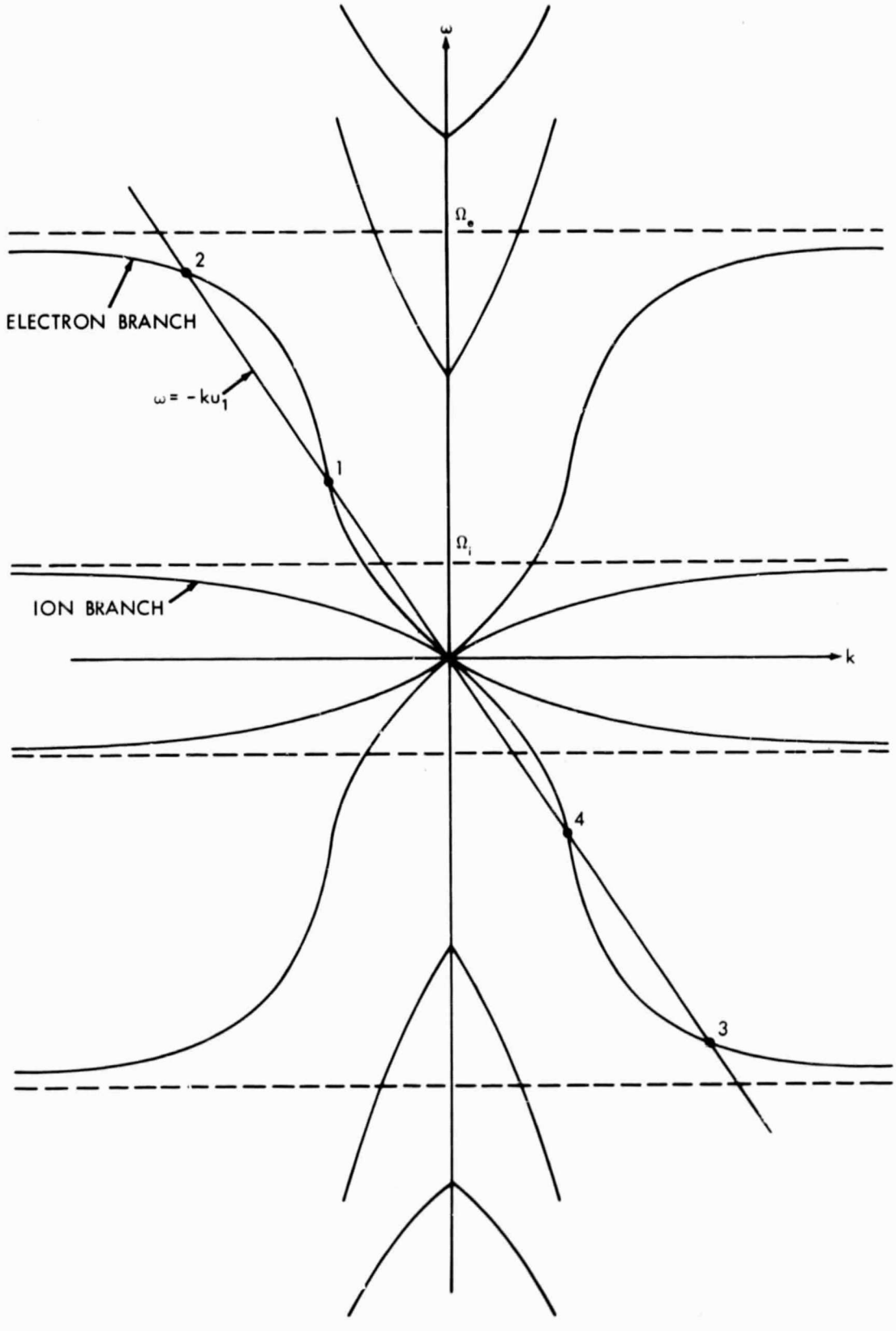

FIG. 3

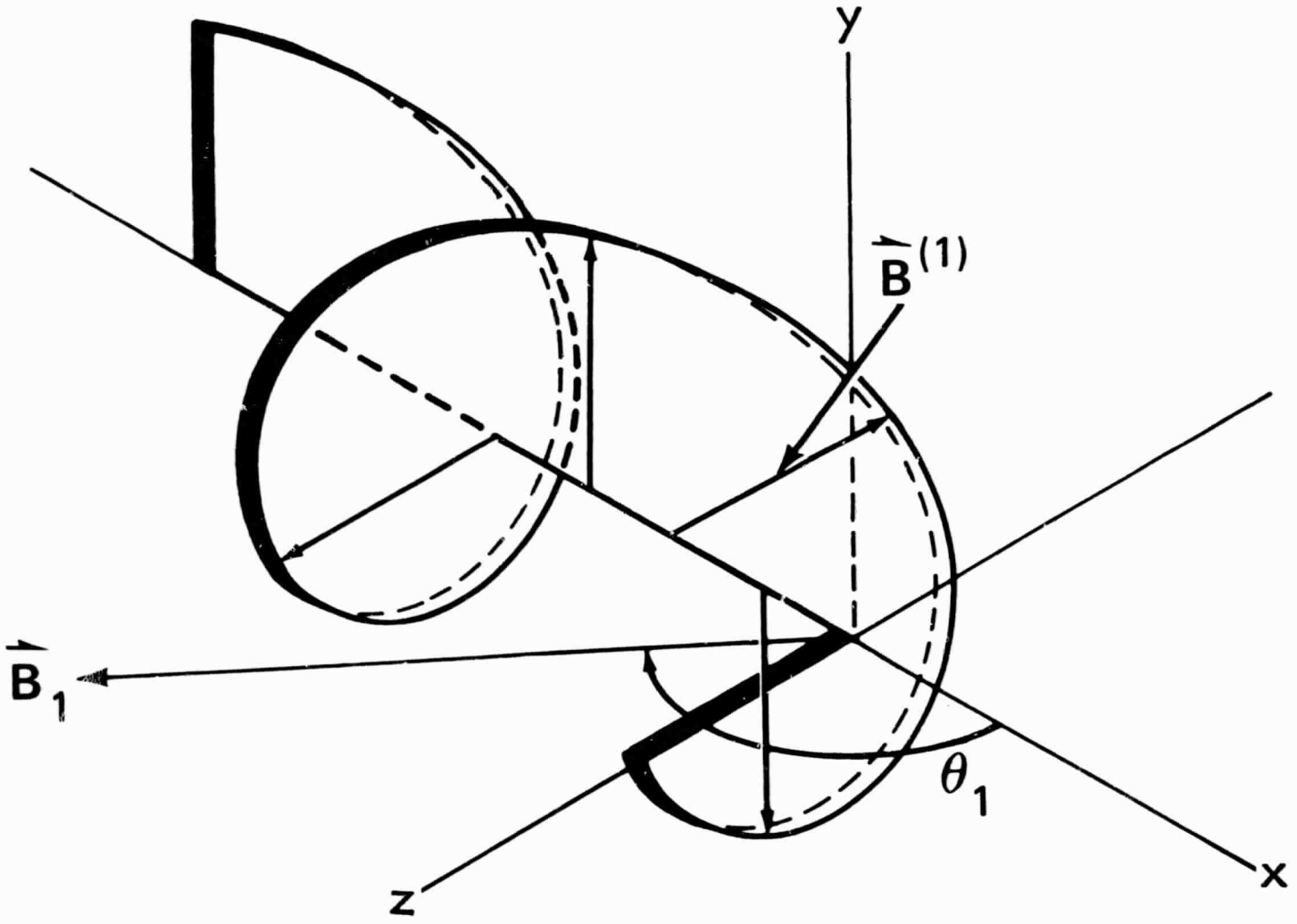

LEFT HAND HELIX

FIGURE 4a

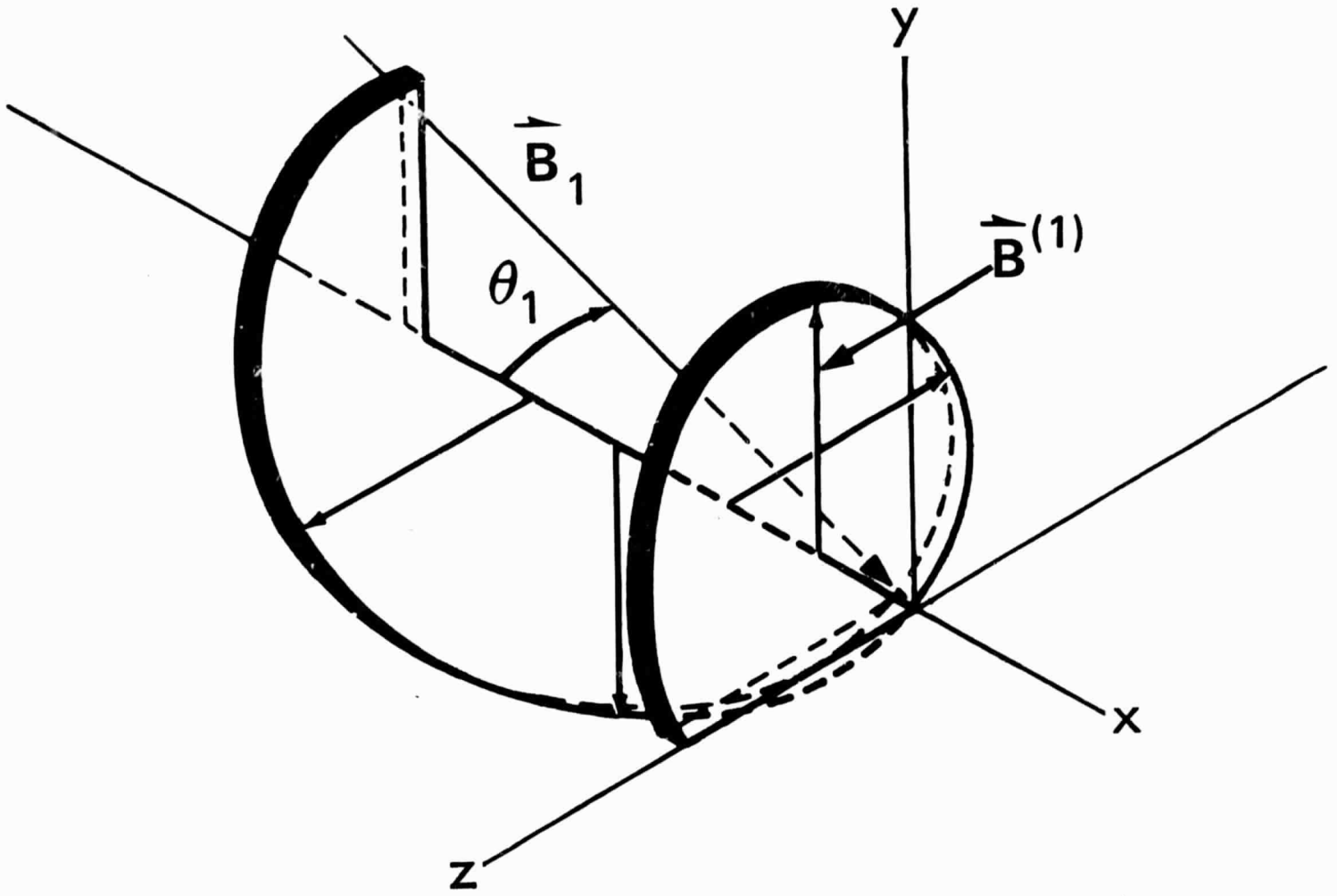

RIGHT HAND HELIX

FIGURE 4b

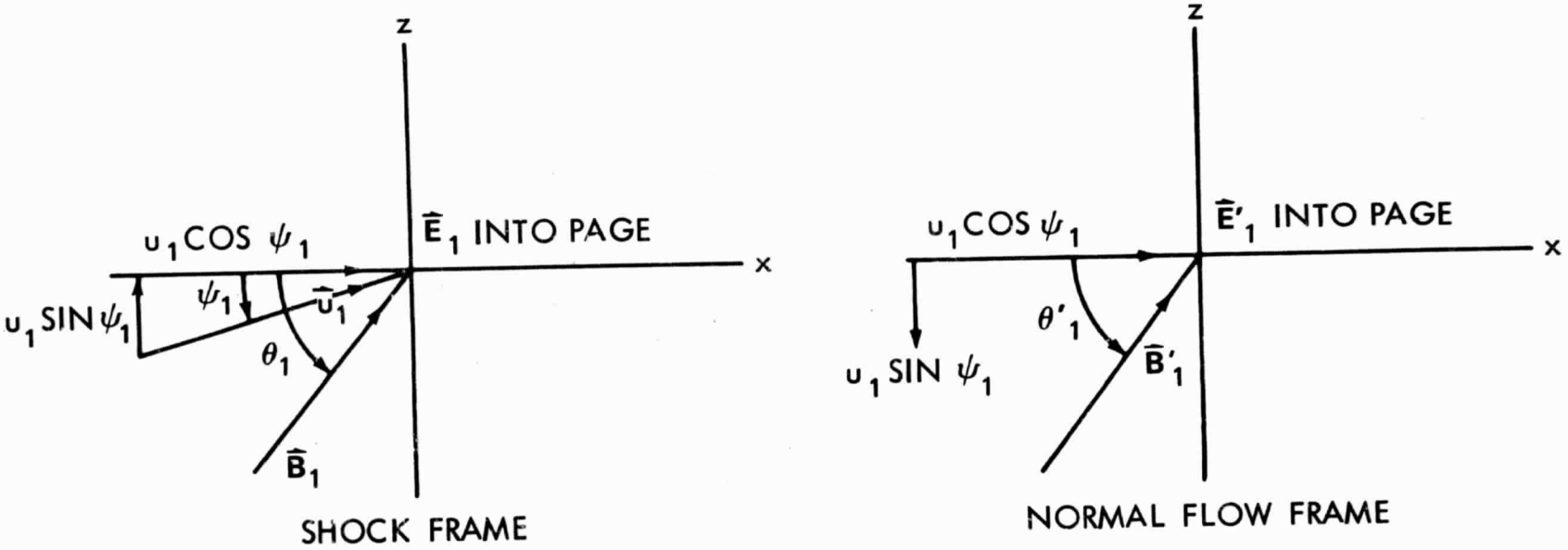
z
x
$u_1 \cos \psi_1$
$\hat{E}_1$ INTO PAGE
$u_1 \sin \psi_1$
ψ_1
$\hat{u}_1$
θ_1
$\hat{B}_1$
SHOCK FRAME
z
x
$u_1 \cos \psi_1$
$\hat{E}'_1$ INTO PAGE
θ'_1
$u_1 \sin \psi_1$
$\hat{B}'_1$
NORMAL FLOW FRAME

FIG. 5

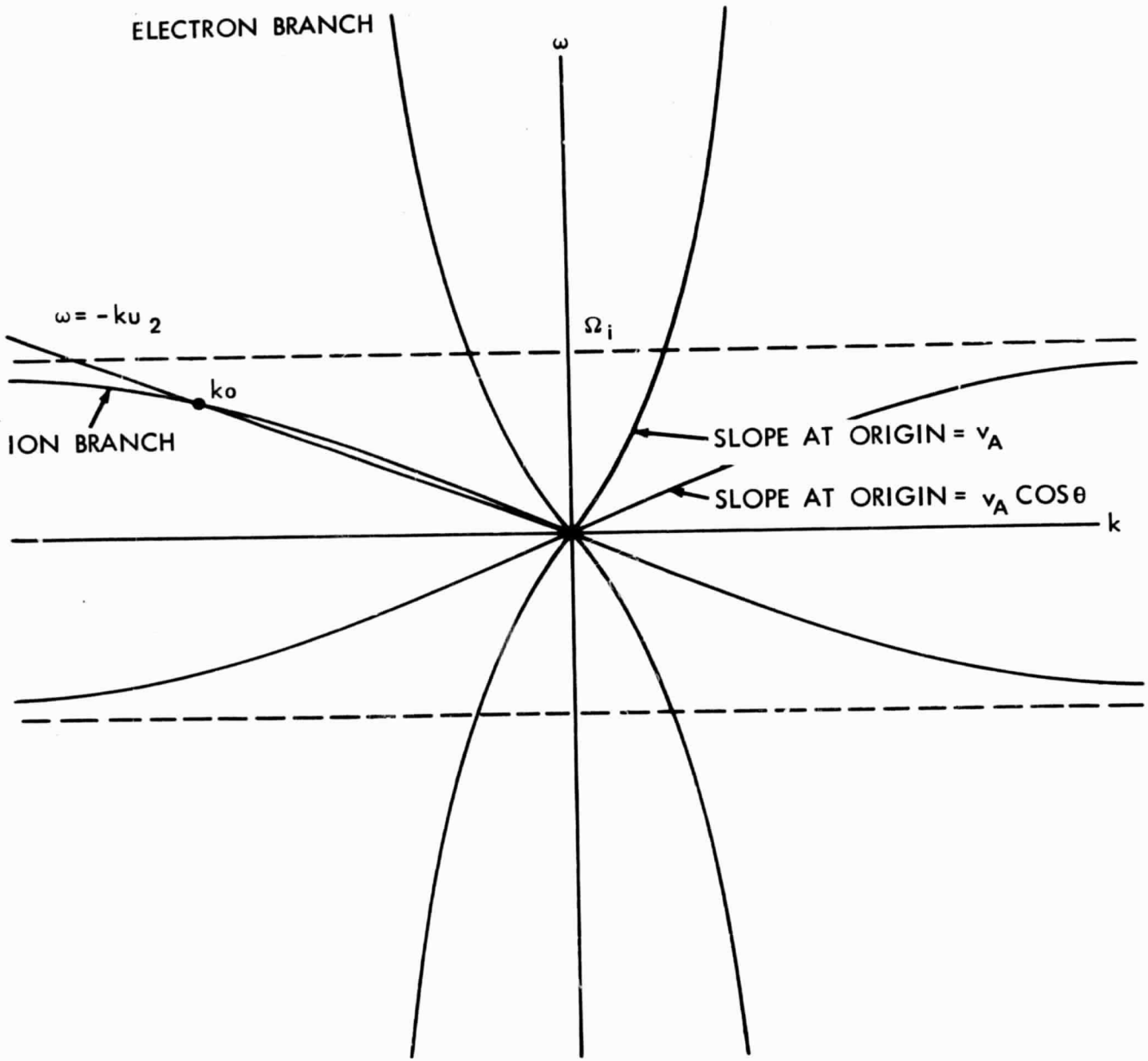
ELECTRON BRANCH
ω
ω = - ku 2
Ωi
ko
ION BRANCH
SLOPE AT ORIGIN = vA
SLOPE AT ORIGIN = vA COSθ
k

FIG. 6